# Thermoreversible Gelation of a Rodlike Polymer

**D. L. Tipton and P. S. Russo***

*Department of Chemistry and Macromolecular Studies Group, Louisiana State University, Baton Rouge, Louisiana 70803-1804*

*Received January 10, 1996; Revised Manuscript Received August 15, 1996*[⊗]

ABSTRACT: Thermoreversible gelation of poly($\gamma$-benzyl-α-L-glutamate) in toluene has been studied by differential scanning calorimetry and by static and dynamic light scattering. For high molecular weights, this system tends to form clear gels when rapidly cooled to low temperatures and more cloudy gels for quenches to temperatures near or slightly above ambient. Differential scanning calorimetry measurements on low-mass polymers show that the melting temperature and also the width of the melting transition depends upon both concentration and type of quench. Gels quenched rapidly to −10 °C melt at lower temperatures, and more sharply, than gels formed slowly at 25 °C. A series of autocorrelation functions, intensity measurements, and visual observations during slow gelation at 30 °C showed that a clear gel formed first, followed by a slightly cloudy gel and partial heterodyning. For visible light at commonly used scattering angles, the apparent fractal dimension of clear and cloudy gels was not dramatically different, a rather extended structure being indicated in either case. Dynamic light scattering measurement during stepwise cooling was used to follow the decrease in apparent diffusion and increase in the gel fraction, as defined on the dynamic light scattering time and distance scales. On melting either clear or cloudy gels, an estimate of the melting temperature could be identified from the power law behavior of the autocorrelation function. The power law regime spanned 3−5 decades of time. Parameters associated with the line shape of the correlation function echoed the results of differential scanning calorimetry on low-mass polymer: a sharp melting transition was observed for the rapidly quenched gel, while the slowly cooled gel melted in a complex fashion over a broader temperature range. These observations reflect the competition between connectivity and phase transitions.

## Introduction

Thermoreversible gelation is one of the most poorly understood aspects of polymer science. Random flight polymers, by virtue of their great flexibility, can easily form multifunctional crystalline or semicrystalline cross-links to stabilize a gel network, so it is at least easy to visualize gelation. It is less clear how rodlike polymers can participate extensively in intermolecular cross-links, and yet rodlike polymers often do gel.[1−6] This is not only a curiosity, but a matter of practical significance. During fiber and film fabrication, rodlike polymer solutions are often quenched into nonsolvents, causing gelation and inhomogeneities that can adversely affect performance. Production of three-dimensional objects from rodlike polymers may be facilitated by polymer gelation, followed by solvent removal. A wide variety of gel structures is available, and the potential exists for new materials processed from them.

Good model systems for thermoreversible gelation are always hard to find. Lacking configurational entropy, rods are even more sensitive to poor solvent conditions than are other polymers. Since its behavior in good solvents is largely understood,[7−23] the helical polypeptide, poly($\gamma$-benzyl-α-L-glutamate), PBLG, is a common choice for studying rodlike polymer gels.[2,3,6,24−33] In this paper, we use differential scanning calorimetry (DSC) and static and dynamic light scattering (SLS and DLS) to explore the wide range of behavior that can occur in PBLG/toluene.

## Background

PBLG is nonionic and very rigid.[8,9] It aggregates end-to-end in toluene, even at high temperatures.[34] When toluene solutions above some critical concentration are cooled, real gels form: samples of reasonable size cease to flow on any reasonable time scale. For example, a 1 $cm^3$ gel will not flow visibly over a period of many years when tilted on its side. If cut with a sharp knife, it will not heal. Miller and co-workers[2,24] suggested that liquid−liquid phase separation takes the lead role in gelation. Structures formed during phase separation were supposed to lose fluidity and thereby stabilize the gel. Optical microscopy confirmed apparently connected structures in *some* PBLG/toluene gels,[25] in PBLG gels in *N,N′*-dimethylformamide, DMF,[27] and in DMF−water mixtures.[26] Evidence from other systems[4,5,35] also validates Miller's suggestion that microphase separation can play a role in rodlike polymer gelation.

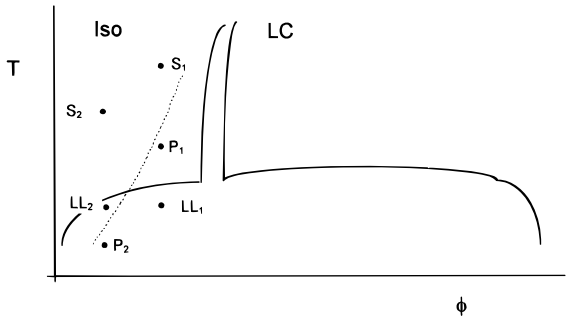


**Figure 1.** Schematic phase diagram for rodlike polymers showing isotropic (Iso) and liquid crystalline phases (LC). The diagonal dashed line shows a hypothesized connectivity transition. See text for the other symbols.

The rodlike polymer phase diagram predicted[36,37] by Flory appears in Figure 1. Isotropic and liquid crystalline phases coexist over a narrow concentration range in good solvents but are widely separated in poor solvents. These general features have been confirmed,[19,20] but actual systems may be much more complex.[29,38] In particular, rods immersed in poor solvents often fail to dissolve. When brought from good solvent to poor solvent conditions, they often gel.[6]

* To whom correspondence should be sent.
[⊗] Abstract published in *Advance ACS Abstracts,* October 1, 1996.

S0024-9297(96)00029-0 CCC: $12.00 

Several facts about PBLG/toluene suggest that phase separation cannot describe the process entirely. Wide angle X-ray diffraction showed diffuse halos from dilute PBLG/toluene gels, and films dried from gels gave only weak reflections.[39] Low-angle light scattering experiments[25] failed to confirm that spinodal decomposition occurred. Thermal transitions are weak (see below). Russo *et al.*[25] hypothesized that entanglements might stabilize the gel phase. Evans and Edwards[40] had advanced a theory wherein concentrated solutions of rods of a finite diameter undergo a jamming effect and cease to diffuse. This purely athermal theory was developed and extended[41] as a model of the glass transition. Since liquid crystals can be formed by evaporating a dilute solution in appropriate solvents, the putative jamming must be subverted by the liquid crystal transition under equilibrium conditions. Self-diffusion studies of PBLG in a good solvent also show that diffusion never ceases in the isotropic regime.[42] Only under nonequilibrium conditions can rod jamming be a plausible mechanism for gelation. The occasional appearance of birefringent regions in aged (several months) PBLG/toluene gels suggests that the gels could indeed be a nonequilibrium state trapped *en route* to full phase separation. Preliminary DLS measurements revealed residual motion in the post-gelation regime,[6] but this need not represent diffusion.[43]

The current study is motivated by one troubling and longstanding observation: the turbidity of a PBLG/toluene gel depends greatly on the temperature and rate of quench. A hot solution rapidly cooled in an ice bath will gel almost instantaneously and scatter just marginally more than the starting solution. The very same hot solution cooled to a temperature near 30 °C will gel slowly and become visibly cloudy. This observation, which is consistent with recent work on PBLG/benzyl alcohol by Cohen and Dagan,[29] was interpreted previously by one of us[25] in terms of the "completeness" of phase separation, with the clear gel produced quickly at low temperature being less completely phase separated than the high-temperature gel (i.e., the clear gel is "pinned" earlier, for whatever reason). Indeed, a clear gel could be made without *any* phase separation at all. Such a process implies the existence of specific interactions among the rods, so that the system can simply convert to a connected network under appropriate conditions. Such networks should not differ physically from chemical gels, which are often modeled by percolation simulations.[44,45] We shall sometimes refer to uniform networks formed as a result of pure connectivity transitions as "percolation networks" to distinguish them from thermoreversible gels generally, which may also include structures formed as a result of incomplete phase separation. In Figure 1, a connectivity transition is superimposed on the Flory phase diagram. The location and even the very existence of the line depend on solvent−polymer[29,38] and polymer−polymer specific interactions. To the right of the dotted line, the system becomes a space-filling, interconnected gel without any change in the local concentration of polymers, except at cross-links. This type of construct has long been used in random flight polymers and covalent gels to describe the competition between gelation and phase separation.[44−46]

Referring again to Figure 1, if a system initially at point $S_1$ (S for "sol") is cooled, it may cross the dotted line to become a gel at point $P_1$ (P for "percolation network"). The actual character of the gel may be determined by kinetic effects. If the connectivity transition occurs rapidly, further cooling will not lead to gross phase separation, although local concentration fluctuations may become amplified and slowed.[47] If the connectivity transition is slow, cooling rapidly to point $LL_1$ (LL for liquid−liquid separation) could lead to phase separation. It is possible to imagine a different situation. Beginning at point $S_2$, we may arrive at point $LL_2$ before crossing the percolation threshold. Depending on whether $LL_2$ lies above or below the spinodal curve, and depending upon the rate of cooling, the mutual friction factor of the polymers, and the strength of the thermodynamic driving forces, it could be possible to reach the point $P_2$ without significant phase separation. In such a case, the connectivity transition would prevent phase separation. A system so prepared could, upon heating to release the specific interactions that stabilize the percolation network, phase separate.[48] Even without heating, a quenched system may slowly find its way to the equilibrium phase-separated state if the forces supporting the percolation network are weak.

Other approaches involving phase separation or other transitions have appeared. Arnauts and Berghmans[49] overlaid glass transition and phase separation plots in their treatment of gelation. Ren and Sorensen[50] have considered the relation between gelation and vitrification more formally. The recent treelike theory of Tanaka and Stockmayer[51] specifically treats the competition between gelation and phase separation. It does not allow for loops but includes other realistic features (e.g., many chains tethered to a common cross-linking site, as in thermoreversible gels of crystallizable polymers). The liquid−liquid part of the phase diagram may acquire a cusp near the intersection with the dotted percolation line. The theory successfully predicts the sudden onset of gelation due to high junction multiplicity and makes solid predictions for the thermodynamic order of the connectivity process. In particular, reversible gelation of polydisperse polymers is a second-order transition, with a finite discontinuity in the osmotic susceptibility that should affect scattering intensity.

The ability to form gels with or without obvious evidence of phase separation makes PBLG/toluene an appealing system to study the competition between phase separation and connectivity. Much has changed since the system was last studied.[25] Correlator advances due largely to Schatzel (see section 2.4.3 of ref 52) enable DLS meaurements over 10 decades of time. There have appeared new scaling interpretations of DLS data from systems near the gel point[53] and a framework for generating the correct ensemble average correlation functions in torpid, "nonergodic" systems.[54] It now becomes tempting to think about thermoreversible gelation as we do about other physical transitions—i.e., to search for the unifying themes. For example, scaling concepts have been applied to polysaccharide gels.[55]

## Dynamic Light Scattering in Gels

This section provides a background for the DLS experiments, which require special precautions at and beyond the gel point. For a detailed treatment, consult refs 54, 56, and 57. In fluid solutions, DLS follows the ebb and flow of spontaneous concentration fluctuations. A spatial Fourier component of the concentration, $c(\underline{q},t)$, is selected by the instrument to match the spatial frequency and direction of the scattering vector, $\underline{q}$, whose magnitude is $q = 4\pi n \sin(\theta/2)/\lambda_0$, with $n$ the solution refractive index, $\theta$ the scattering angle, and $\lambda_0$ the incident wavelength *in vacuo*. Data are usually gathered under homodyne conditions[58,59] and analyzed under the assumption of a Gaussian-distributed light

field with the aid of the Siegert relation:[52]

$$g^{(2)}(q,t) = \frac{\langle I(q,t)\cdot I(q,0)\rangle}{\langle I(q,0)\rangle^2} = 1 + f|g^{(1)}(q,t)|^2$$

The angular brackets indicate a time average, and $g^{(1)}(q,t)$ is the normalized electric field autocorrelation function, $\langle E^*(q,t)\cdot E(q,0)\rangle/\langle E(q,0)\rangle^2$. For a single, simple diffuser, $g^{(1)}(q,t)$ decays with lag time, $t$, as an exponential: $g^{(1)}(q,t) = \exp(-\Gamma t)$, with a decay rate $\Gamma = q^2 D_m$, where $D_m$ is the mutual diffusion coefficient. The instrument parameter, $f$, lies between zero and unity, depending mostly on the number of coherence areas detected.[60]

An ideal gel could be made by chemically cross-linking polymers that are already dissolved at a concentration in the strongly overlapped regime, without otherwise altering the structure. The scattering from such a gel would be virtually identical to that of the nascent polymer solution. The system would differ from a concentrated polymer solution mainly in that some of the polymers cannot really diffuse; their *self*-diffusion is zero. Nevertheless, there still occur fluctuations in the local, instantaneous concentration, and the apparent mutual diffusion coefficient from DLS is related to the gel modulus.[43]

Real gels may exhibit complex DLS behavior. Slow fluctuations may exist, often associated with large inhomogeneities, high scattered intensity, and strong angular dependence. There are two approaches.[56,57] One may assume the inhomogeneities to be truly immobile and let them serve as a heterodyne source.[58,59] In addition to the dangers implicit in the assumption, one must also ensure that the reference beam provided by the inhomogeneities is much stronger than the scattering arising from the fluctuating component. The other option is to treat the gel as a nonergodic medium. This approach recognizes that each small region of space has an average concentration, and fluctuations about that average are restricted by the gel structure, so that a time average from a single region is not representative. At a particular point in the scattered field, the electric field is no longer a random, zero-mean quantity. Many such subvolumes must be sampled in order to validate the application of the usual Siegert relationship.

In the "short-cut" sampling method,[54,57] only one time-averaged autocorrelation function, $g_T^{(2)}(q,t)$, is carefully measured, ideally by first selecting a "speckle" in the scattered field having average brightness. The true ensemble-averaged autocorrelation function, $g_E^{(1)}(q,t)$, is constructed using statistical properties of the scattered radiation, compiled from comparatively rapid intensity measurements made on many speckles. To bring different speckles into the small area observed by the detector, the sample is moved slightly. In the present work, we instead follow the "brute force" method,[54] wherein $g_T^{(2)}(t)$ is measured many times from different speckles and averaged, as described in the following section. This slower method is preferred for systems where the "frozen" intensity component is not really permanently frozen, as in gels near the transition point. Most of the data are presented in terms of the ensemble-averaged, second-order autocorrelation function, $g_E^{(2)}(q,t)$. As the zero-mean, Gaussian properties of the scattered field are preserved by the multispeckle averaging process, $g_E^{(2)}(q,t)$ obeys a Siegert relationship: $g_E^{(2)}(q,t) = 1 + f|g_E^{(1)}(q,t)|^2$.

## Experimental Section

**Differential Scanning Calorimetry.** A Seiko DSC 120 was used, which is perhaps 10 times more sensitive than calorimeters commonly used for bulk polymers. A low molecular weight PBLG ($M$ = 16 000, Sigma No. 85F-5031) was studied to increase concentration and sensitivity. Bulk solutions of various concentrations were melted at ~90 °C and quenched to either −10 °C or ca. +25 °C. The heating rate was 2 °C/min. Additional details appear in the supporting information.

**Light Scattering Sample Preparation.** The preparation of clean gel samples is described in the supporting information. Briefly, since PBLG aggregates in toluene, samples were dissolved in DMF for clarification and then exchanged back to toluene. Sample clarity was checked by viewing the scattered and refocused light at about 100 times magnification using the observation port on the DLS instrument.

**Light Scattering Protocol.** The light scattering setup consisted of a vertically polarized helium−neon laser (15 mW, Spectra Physics SP-124b), photomultiplier tube (EMI 9863b), and an ALV-5000 correlator. The temperature was maintained to ±0.01°C with a Hart Scientific model 2100 controller. Multiple runs were always measured, using the symmetric normalization scheme.[52] For samples near or beyond the gel point, the cell was rotated a random amount between runs, either by hand or with a stepping motor (model MCMSE from Ludl Electronic Products). The duration of the individual runs should exceed greatly the correlation time of the slowest process. In gels, this can be difficult to judge. The best method is to ensure that the coherence parameter (after ensemble averaging when necessary) matches that determined from a strongly scattering, ergodic sample using the same instrument settings. Visual inspection of each individual run enabled deletion, before averaging, of any measurement that might have been corrupted by dust or data overflow errors. Very few runs had to be deleted. For fluid samples, a simple average was constructed. In principle, fluid samples can be measured in a single, long run. Breaking the acquisition into multiple runs limits the time scale of the processes that can be studied, but offers other advantages (among them, identification of outlier data and a population estimate of uncertainties). The proper ensemble average for nonergodic samples was performed using a method suggested by ALV for converting the multiple $g_T^{(2)}(q,t)$ data sets to a single estimator of $g_E^{(2)}(q,t)$. The ensemble averaged data for most of this paper were the result of 20−200 runs; this selection is justified below.

## Results and Discussion

**Differential Scanning Calorimetry.** The absence of measurable enthalpies in previous studies,[2,25] unlike the PBLG/DMF/$H_2O$[61] and PBLG/benzyl alcohol[3,28,32] systems, was partly responsible for speculation that gelation in PBLG/toluene might be due to entanglements. This now seems unlikely, as discussed above. If entanglements are not responsible for gelation, a DSC signal would be reassuring. DSC transitions *are* evident in the present study. To enhnace sensitivity for quantitative measurements, a more highly soluble low-$M$ sample (PBLG-16000) was studied. The temperature of the first change in the derivative curve was identified as the beginning of the peak and the melting temperature. For the gels made at 25 °C, $T_{melt}$ is fairly uniform; see Figure 2. Quenching to −10 °C leads to lower melting temperatures that decrease with increasing concentration. The error bars from repeat runs indicate better reproducibility for the −10 °C gels than for the 25 °C gels. Reproducibility was quench rate dependent in other DSC studies.[62] Guenet and McKenna[63] reported that isotactic polystyrene/decalin gels which were melted and re-formed by rapidly quenching to 0 °C have more poorly defined melting endotherms than those allowed to form at 14 °C. This contrasts with our PBLG results. The gels studied by Guenet and

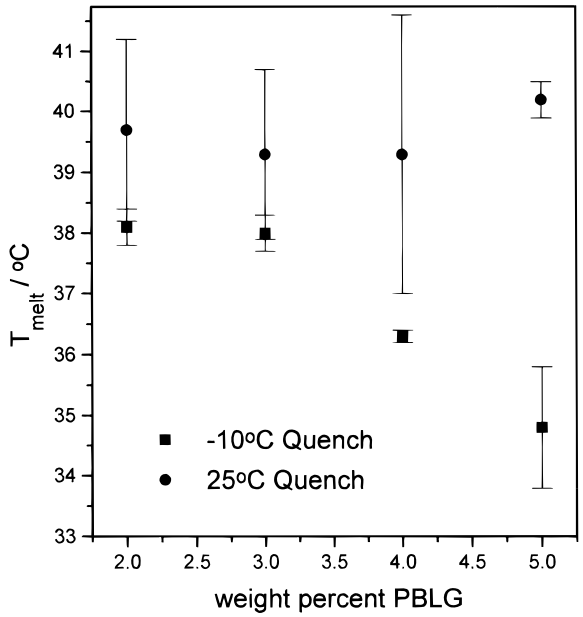


**Figure 2.** DSC melting temperatures for gels made under both quench conditions, at various concentrations of PBLG-16000 in toluene.

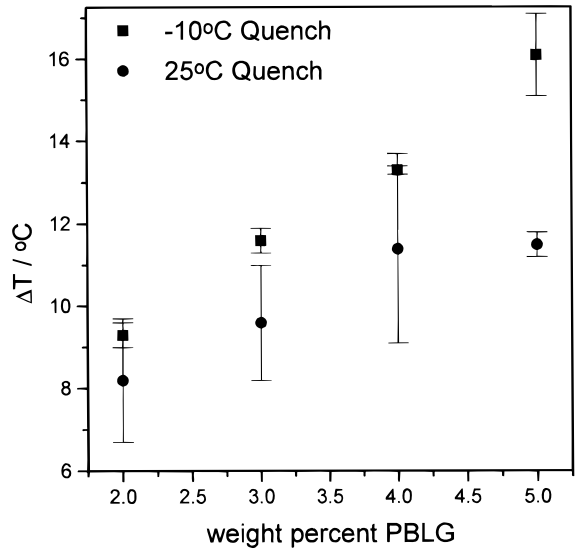


**Figure 3.** DSC peak widths for melting of gels made under both quench conditions, at several concentrations of PBLG-16000 in toluene.

McKenna are believed to be formed by solvent bridging between the polymers and it is hypothesized that by rapidly quenching the sample, the network is "far from being perfect." (ref 62, p 13) The large uncertainties for the slowly quenched gels in Figure 2 may indicate that the polymer rods are at different stages of phase separation. Care was taken to ensure that the aging time was kept constant for all concentrations and all runs.

The temperature at which the derivative signal returned to its baseline was chosen as the end of the peak. Figure 3 shows that the DSC transitions broaden as the polymer concentration increases at either quench temperature. Also, the −10 °C quench gels melt over a slightly wider range of temperatures, but with better reproducibility, than do the 25 °C gels. Figure 4 shows the enthalpy of melting in mJ/mg of polymer as a function of concentration (w/w %). This would be more accurately measured upon cooling. Only the results for the −10 °C gels are shown; large uncertainties obscure

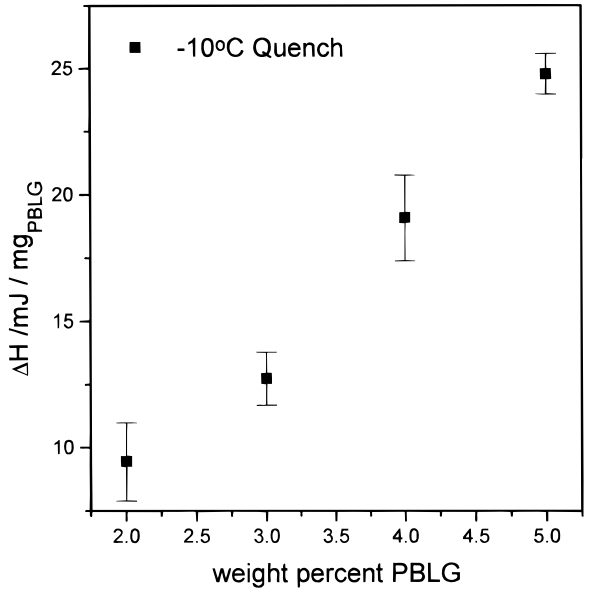


**Figure 4.** Enthalpy of melting for gels made by rapid quench to −10 °C, at various concentrations of PBLG-16000 in toluene.

any conclusion for the 25 °C gels. The enthalpy for the −10 °C quench gel increases linearly with concentration. At a concentration of 0.49 ± 0.32%, the enthalpy of melting is zero. This may indicate the critical concentration, $c^*$, for gel formation. Even though the error is large, the measured $c^*$ is surely lower than $c^* = 5.44 \pm 1.0\%$ calculated from intrinsic viscosity[64] ($c^* = [\eta]^{-1}$) and much lower than $c^* = 20\%$ calculated from the radius of gyration ($c^* = 3M/4\pi N_A R_g^3$ where $N_A$ = Avogadro's number and $R_g$ = rod length/$\sqrt{12}$).[65] The small $c^*$ is probably due to end-to-end aggregation of PBLG in toluene.[34] These DSC results show conclusively that there is an enthalpic interaction. This is not a sufficient condition for a connectivity transition, but it is a necessary one in a system lacking covalent links or permanent entanglements. Although all the DSC studies used highly turbid, low-$M$ PBLG gels, weak endothermic transitions were also evident on melting gels of the higher-$M$ PBLG samples used for light scattering. A more sensitive calorimeter would be desirable for quantitative work on high-$M$ gels.

**Overview of Light Scattering Experiments.** Five different light scattering experiments were performed.

(1) A kinetic experiment followed changes in intensity and correlation functions after cooling from 90 to 30 °C.

(2) Angular dependence of scattered intensity was measured for both clear and cloudy gels.

(3) The formation of a cloudy gel on cooling was studied in a stepwise temperature series. At each temperature, brute force ensemble average correlation functions were taken at various angles. The dependence of $D_m$ on $T$ was obtained, along with other parameters, such as apparent gel fraction.

(4) A cloudy gel was melted in small temperature steps. At each step, the ensemble-averaged correlation function at a single angle was generated by the brute force method.

(5) Step 4 was repeated for a clear gel.

**Kinetic Light Scattering.** A 0.01 g/mL solution of PBLG-66000 in toluene was heated to 90 °C and then placed in the light scattering instrument ($\lambda_0 = 632.8$ nm, $\theta = 60°$), where the temperature was held constant at 30 °C. Intensity and the apparent coherence parameter, $f$, from single, temporally averaged correlation functions were taken at 10 min time intervals over a 12 h period.

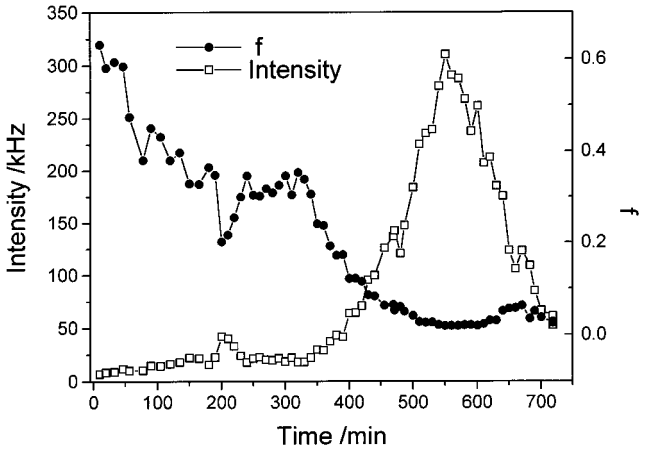


**Figure 5.** Intensity and apparent coherence parameter for 0.01 g/mL of PBLG-66000 in toluene, as a function of time since cooling from 90 to 30 °C. Data were collected at $\theta = 60$ °C.

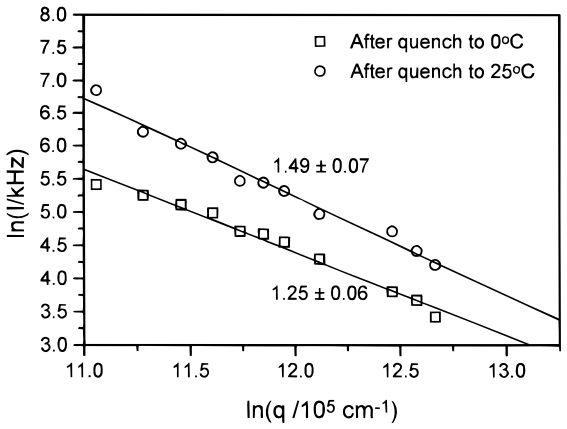


**Figure 6.** Double log plots to obtain apparent fractal dimensions, shown for two quench conditions producing clear and cloudy gels.

This entire experiment was repeated four times. A sample trace is shown in Figure 5 from the first attempt. Two peaks in intensity are clearly visible. The first occurs 200 min after quench—i.e., at $t_q = 200$. Inspection of the sample at this time revealed that a clear gel had formed. The sample was tilted on its side for about 2 min and appeared solid. This qualitative indicator of the gel transition depends upon the size and strength of the sample, but gelation in any conventional sense of the word had certainly occurred. The sample was reinserted in the instrument, and the intensity decreased to nearly the pregel value. The intensity began to increase again after $t_q = 350$ min total time, reaching a maximum value at $t_q = 550$ min, followed by another decrease. It is not certain whether further long-time oscillations would have been observed, as in networks of actin filaments.[66] After 720 min the sample was removed. The gel had changed from clear to slightly turbid. A power meter placed at 0° scattering angle showed no large decrease in transmitted light, indicating that the decreases in scattered light after about 220 and 550 s were not due to absorption or turbidity.

The intensity changes in Figure 5 are mirrored by opposite trends in the apparent coherence parameter, *f*. This was generally true in the three repeat runs, too (not shown). However, the amplitude of the increase in intensity and associated decrease in apparent coherence varied from run to run. The time at which these events occurred did not vary. The probable explanation is that, at the end of each of the four runs, the gels all had a nearly stationary speckle pattern. The overall reduction in the apparent coherence and increase in intensity depended upon whether the final scattering volume produced a bright or a weak speckle at the detector, which was set for moderately high coherence. In the run shown in Figure 5, the system was initially completely homodyne ($f \sim 0.65$, typical of strongly scattering, fluid solutions for the particular detector settings in use). At the end of the gelation, reasonably good heterodyne efficiency was achieved (*f* decreased to ~0.02). Except for the gels at $t_q = 0$ and $t_q = 720$ s, the correlation functions used to obtain Figure 5 (and the three repeats) were measured under mixed heterodyne–homodyne conditions. Additionally, the intensity is actually increasing during some of the runs. This is why the *f* values have been referred to as "apparent". Under these conditions, correlation times cannot be used quantitatively, but inspection showed that most of the decay remains in the 1–10 ms time scale throughout the transition. Normalized, first-order correlation functions for $t_q = 0$ (computed as a pure homodyne measurement, using the Siegert relation) and $t_q = 720$ s (computed under the assumption of a strong, stationary local oscillator[58,59]) showed a somewhat slower relaxation for the gel at 720 s, in addition to emergence of a very slow decay. In two of the four repeat gelations, the apparent coherence parameter decreased only by about half as much as shown in Figure 5; gels generally cannot be trusted to provide a good heterodyne source for themselves. Despite their mixed homodyne–heterodyne nature, these kinetic experiments showed that a clear gel formed at early times at a high temperature can evolve into a more cloudy one later. The intensity increased just modestly upon formation of the clear gel. One could argue that the small intensity bump (at about 200 s in Figure 5) results from looking at a weak speckle at some time after formation of a turbid gel. It is the visual observations that the system is clear at this time, plus the consistency with which the small bump is observed, that suggest a two-step process instead. Not even one bump would be expected for a simple connectivity transition. However, the thermodynamic theory of Stockmayer and Tanaka does predict a weak increase in intensity for the connectivity transition for a polydisperse system, which PBLG/toluene certainly is due to aggregation and the intrinsic distribution of the PBLG molecules.

**Angular Dependence of Scattered Intensity.** The scattered intensity can provide important clues to the structure of the gels. A combination of light and neutron or X-ray instruments is usually required to characterize all the important structural scales.[67] Although PBLG gels have been measured individually by these methods,[6,25,29,68–70] no wide-range scattering envelope has been obtained. The present paper does not remedy this problem but simply addresses whether or not clear and cloudy gels differ in their *q* dependence for scattering of visible light. Measurements were conducted repeatedly by cooling a gel from 90 to either 25 or 0 °C. Figure 6 shows typical results, obtained over the range $32 < q^{-1}/\text{nm} < 210$. The low values of the power law slopes indicate a rather extended, "open" structure for both gels, perhaps a bit more so for the clear gel. The cloudy gel, with its very slightly larger power law slope, may be a late attempt at phase separation by a system that is substantially formed as a gelatinous solid by a process not involving phase separation. Compared to the process initially imagined by Miller,[2,24] the sequence of events is reversed. However, one should not generalize these results. They

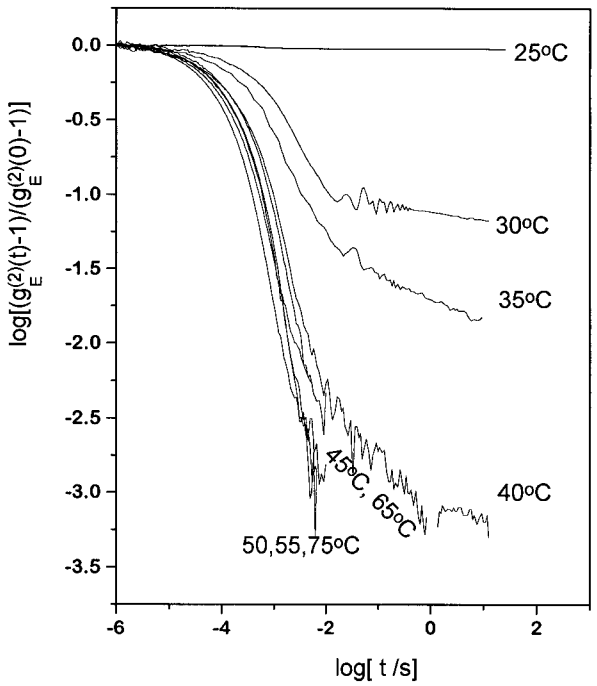


**Figure 7.** Double log plots of ensemble-averaged correlation functions during a stepwise series of decreasing temperatures for 0.005 g/mL of PBLG-91000 in toluene at $\theta = 90°$.

show what *can* happen, not what always happens. In other solvents (e.g., wet DMF) it is certain that phase separation happens first. At other concentrations, cooling rates and molecular weights in PBLG/toluene, the same is true. Variability in gel conditions probably explains the different power law slopes observed.[6,68,70]

**DLS Experiments during a Stepwise Series of Decreasing Temperatures Leading to a Cloudy Gel.** The experiments in this section were undertaken in order to more nearly approximate equilibrium conditions and give stable baselines for DLS. A molten solution of PBLG-91000/toluene at 0.005 g/mL was placed in the light scattering device at 90 °C. Measurements were taken at several angles in the range $30° < \theta < 135°$. The temperature was lowered by 5 deg, followed by an equilibration time of at least 10 h, and then the measurements at multiple angles were repeated. This procedure continued until a final temperature of 25 °C was reached. The angle dependent aspect of this study is not possible for a quickly forming clear gel and would have been challenging to perform during the already described kinetic quench to 30 °C.

Figure 7 shows the second-order correlation functions at one scattering angle, $\theta = 90°$, individually normalized by the value extrapolated to zero lag time to account for the different optical settings used. As the temperature is reduced, the correlation functions decay more and more slowly until, at $T = 25$ °C, there is almost no decaying portion in the measured time domain. These results can be used to follow the gelation process. One definition of a gel is a dilute system that does not flow.[71] It is not too big a stretch to equate the absence of flow with the absence of diffusion for at least some of the polymers present in the system. To use such a definition, both distance and time scales associated with flow (or diffusion) must be given. A large tub of gelatin might "flow" when turned on its side, whereas a sample of the same constitution might never flow out of a fruit cup. The distance scale appropriate to Figure 7 is $2\pi/q \approx 300$ nm. The fraction gelled, $G$, on a particular time scale is given by $(g^{(2)}(q,t) - 1)^{1/2}$. Choosing 1 s as the

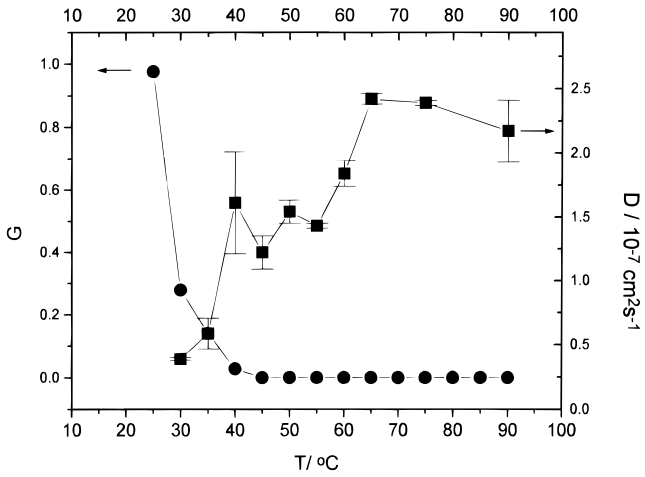


**Figure 8.** Apparent gel fractions and apparent diffusion coefficients. Gel fractions were derived from the correlation functions in Figure 7, as a function of temperature. The "gel" is defined at a 1 s time scale and, on the light scattering distance scale, at about 300 nm. Diffusion coefficients come from multi-angle data collected along with the runs shown in Figure 7; see text.

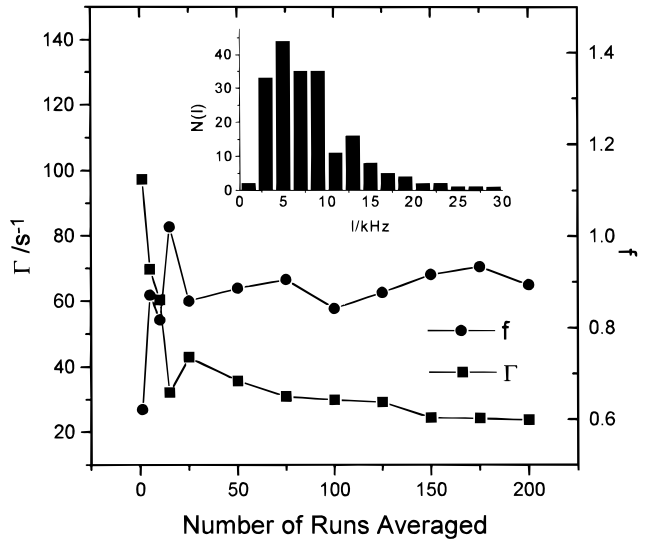


**Figure 9.** Convergence of decay rate and coherence factor with the number of runs included in the ensemble average. Inset: distribution of intensity.

time, the result is as shown in Figure 8. The 1 s limit is about as long as the present data can support, due to the acquisition time of each individual run in the brute force averaging of the 20−40 runs at each temperature. To demonstrate that the total number of correlation functions is sufficient, Figure 9 shows how $\Gamma$ and $f$ depend on the number of runs averaged for the worst case, a fully formed cloudy gel. After about 50 runs, each of duration 180 s, the decay rate is fairly steady, and the coherence parameter, $f$, approaches 0.9, the value obtained with an ergodic system, polystyrene in toluene, for the same instrument settings. The distribution of intensities $N(I)$ (Figure 9, inset) has the expected form[52] for a single random process, consistent with the high-coherence detector settings used, which did not subtend multiple speckles at one time. A 1 s time scale and 300 nm distance scale are far shorter than used in visual assessments of gelation, such as tilting a 1 mL sample to observe flow within 1 h time period. Both clear and cloudy PBLG/toluene gels qualify according to such conventional criteria; as already mentioned, samples remain inverted for many years without any sign of flow. Nor are the gels easily broken

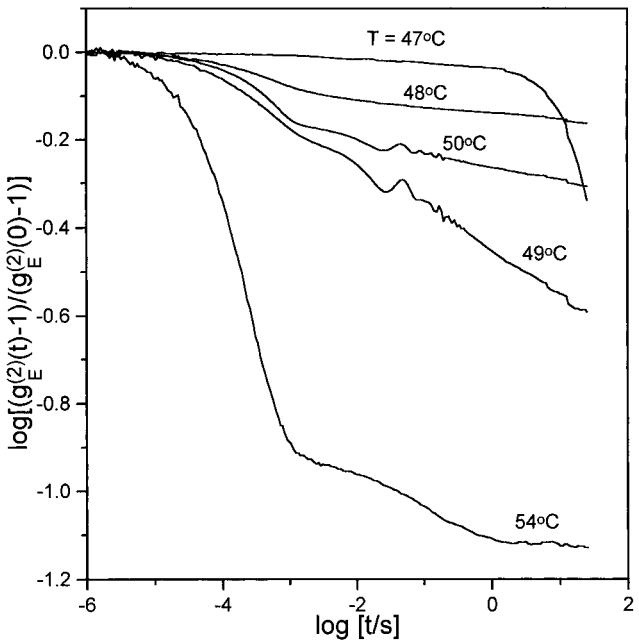


**Figure 10.** Double log plots of the autocorrelation functions for 0.005 g/mL of PBLG-91000 in toluene, collected at $\theta = 90°$ as the temperature is stepwise raised through the melting transition of a cloudy gel.

by shaking. Figures 7 and 8 merely represent these facts using DLS. The mutual diffusion coefficient, obtained[72] as the initial slope of the average decay rate of the correlation functions plotted against $q^2$, decreased almost monotonically with temperature during this stepwise cooling experiment. The decrease began at about 60 °C, well ahead of the increase in $G$, as shown in Figure 8. Such a large decrease cannot be accounted for by changes in toluene viscosity with temperature and implies that increased aggregation accompanies temperature reduction and precedes gelation.[34] Although the trends demonstrated in Figures 7 and 8 herald gelation, the temporal and spatial ambiguity implicit in flow-based or diffusion-based definitions are powerful motivators to explore better methods to identify gels. In the next section, undercooling and sample history effects are minimized by studying the melting of gels rather than their formation.

**DLS upon Melting of a Cloudy Gel.** Measurements at a single scattering angle were taken at ~0.2 deg increments with brute force averaging of 40−50 runs. The individual time-averaged correlation functions had a duration of 180 s; processes occurring on a time scale longer than about 100 ms will not be measured with high accuracy. Equilibration time between the 0.2 deg steps was 3 h. A scant few of the correlation functions appear in Figure 10. Overall, the correlation functions display more mobility at high temperatures than at low, which is expected. However, the behavior is not completely monotonic; the correlation function at $T = 50$ °C lies above that at $T = 49$ °C, qualitatively indicating a higher gel fraction at the higher temperature. The correlation function at 49 °C obeys a power law over 5 decades of time, marred only by a ripple with a frequency of about 20 Hz. Although it is possible to generate ripples by incorrectly setting the correlator's scaling facility, we believe the oscillation is a real consequence of weak acoustic or mechanical excitation of a very soft viscoelastic system near the gel point. This phenomenon, seen previously,[24] can be exploited for measurements of gel moduli.[73] We did not pursue this possibility, as the cylindrical cells with round bottoms that were used do not provide a convenient boundary condition for the analysis. The power law behavior was not seen in the correlation functions collected as the temperature was lowered leading to the formation of this gel. This may be due to temperature steps (5 deg) that were too large, or to kinetic effects (supercooling) despite the long waits between temperatures. The power law slope in this region is $-0.095 \pm 0.001$, considerably smaller than the $-0.27$ reported by Martin.[53] Unlike other studies, the power law does not extend beyond the gel point but exists only over a 0.4 deg temperature range. In the work of Martin, prior to the gel point, the long-time correlation function relaxes according to a stretched exponential:

$$g^{(2)}(q,t) - 1 = \exp[-(\Gamma t)^b]$$

The stretching parameter, $b$, was found to be 0.67 for a chemically covalent network of silica particles. For a covalent polymer gel of PMMA,[74] $b$ was $0.26 \pm 0.02$. In the present experiment, there is only a hint of truncation, occurring at $T = 47$ °C (see Figure 10), which is really on the wrong side of the transition for additional motions to appear. This again indicates the nonmonotonic melting behavior of the cloudy gel. Perhaps the measured correlation functions do not extend to long enough lag times to exhibit the stretched exponential tail at other temperatures. Improvements would come at a considerable price using a conventional DLS instrument. Correlation functions simultaneously measured at multiple speckles, as with a pixel-type detector,[75] would be more efficient at long sample times.

Correlation functions are commonly converted into decay spectra using Laplace inversion algorithms,[76] such as the popular CONTIN.[77,78] It is supposed that the electric field autocorrelation function can be fitted as $g^{(1)}(t) \sim \int_0^\infty d\Gamma\, A(\Gamma) \exp(-\Gamma t)$ where the $A(\Gamma)$ function represents the amplitude associated with an exponential decay with rate $\Gamma$. Akin to a weighted sum of exponentials, such a form will fit most monotonically decaying data, including the correlation functions measured here. CONTIN applies different levels of smoothness to the solution, effectively tying together nearby "grid points" at which $A(\Gamma)$ is estimated. The program uses statistical parameters to choose, supposedly, the smoothest distribution consistent with the data. Both CONTIN and another Laplace inversion algorithm (a smoothed version[79] of exponential sampling[80]) were applied to several data sets. For example, using 60 grid points, the chosen CONTIN solution to the power law data of Figure 10 (at 49 °C) included six peaks spanning the frequency regime $10^{-4}$ to almost $10^6$ Hz. Amplitudes in the low-frequency regime were poorly estimated in the chosen solution. Typically, the EXSAMP algorithm gave a similar but less detailed, more conservative distribution than the chosen CONTIN solution. The several CONTIN distributions were not particularly stable to changes in the smoothness parameter. Since there is no theoretical basis for a sum of exponentials anyway, the Laplace inversion analysis was abandoned. Still, some way of following the trends with temperature is needed.

It was decided to apply the very flexible stretched exponential form to the *early* part of the autocorrelation functions. The same criticism just leveled at Laplace inversion—namely that there is no theoretical basis—still applies, but at least the number of parameters is reduced. The early parts of the correlation functions were found to follow the stretched exponential form, with $b \approx 0.67$ at temperatures above the gel point. At temperatures below the gel point, $b$ decreased to 0.45

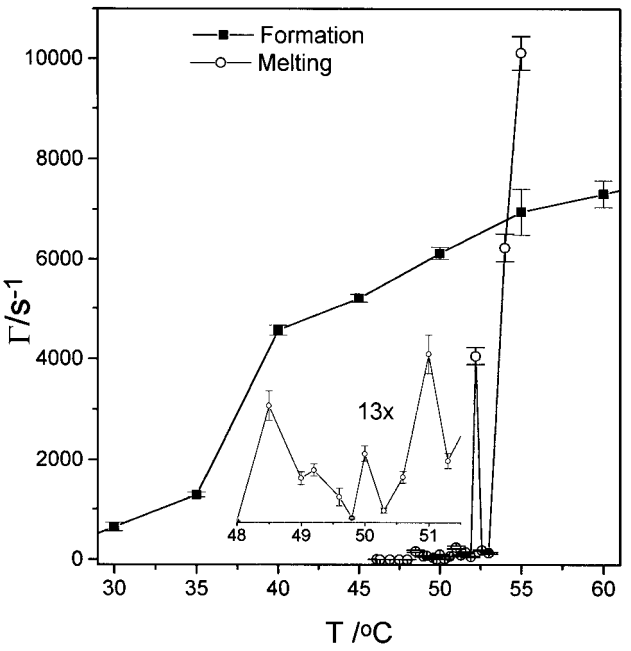


**Figure 11.** Decay rates from stretched exponential fits to the early part of the correlation functions as a function of temperature for stepwise lowering and raising of the sample, respectively, to form and melt the gel. The inset shows the melting behavior on an expanded scale from 48 to 51.5 °C.

± 0.11. The stretched decay rate, Γ, is another indicator of the gel melting transition. This parameter was determined throughout the melting transition, and also for the data of the previous section on equilibrium formation of the cloudy gel. The stretched exponential decay rate exhibits about 14 deg hysteresis; see Figure 11. The Γ parameter is not monotonic on melting. Small fluctuations begin at 48.5 °C, followed by a large increase at 52 °C. The rapid decay at 54 °C corresponds to an ergodic correlation function and represents the onset of macroscopic flow, as observed by tilting. According to Γ, the gel melts over a temperature range of 5.5 deg (i.e., from 48.5 to 54 °C). The gel melting transition indicated by Γ is broader and occurs at a higher average temperature than that indicated by power law behavior. The power law behavior is a more definitive melting criterion, but the transition indicated by Γ corresponded more closely to visual observation. The single exponential cooperative diffusive mode in the early times reported by Martin was not observed. Its absence may be due to the polydispersity of the polymer aggregates at even the highest temperatures, or to the fact that our polymer molecules diffuse more slowly than Martin's monomers, so that cooperative diffusion overlays modes associated with the gel.

**DLS upon Melting of a Clear Gel.** Brute force ensemble averages of 50 individual runs, each of 180 s, are shown in Figure 12. Data at lag times exceeding about 100 ms become progressively less reliable. The coherence parameter, after averaging, approached the norm for the optical settings in use. As shown by the inset, a power law regime extending over almost 3 decades of time is found at 49 °C with a negative slope of 0.113 ± 0.003. The slope slightly exceeds that measured for the cloudy gel (Figure 10) but remains well below the expected[53] 0.27. A more extended power law regime might have been found at a temperature between the measurement steps of 1 deg. The power law regime is truncated by a downturn of the correlation function. The downturn appeared to have a stretched exponential form,[72] as predicted.[53] However, the lag

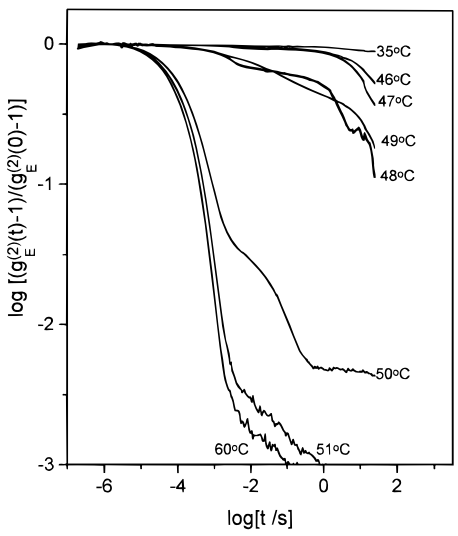


**Figure 12.** Double log plots of the autocorrelation functions for 0.005 g/mL of PBLG-91000 in toluene, collected at $\theta = 90°$ as the temperature is stepwise raised through the melting transition of a clear gel.

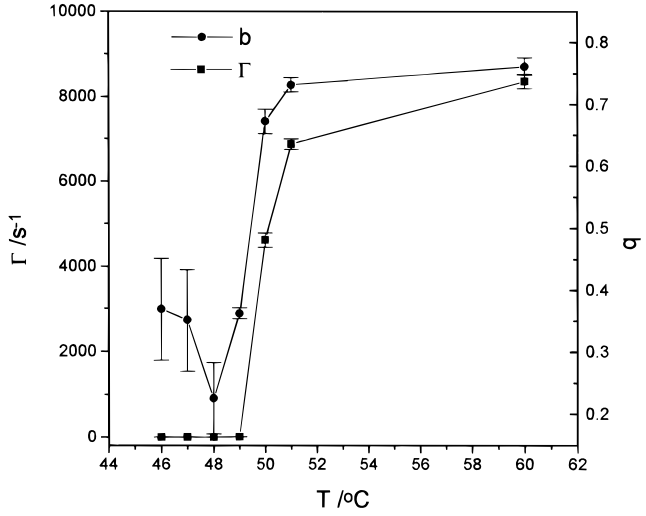


**Figure 13.** Stretched exponential fitting parameters for the early part of the correlation functions of Figure 12 (clear gel; stepwise melting).

times are an appreciable fraction of the total acquisition time, so judgement on this point is reserved. The *initial* part of the correlation function was fitted to a stretched exponential, as for the cloudy gels. Unlike the cloudy gel, the clear gel melted monotonically with ergodic behavior beginning at 50 °C. Both stretched exponential fitting parameters, Γ and *b*, for the early part of these functions increase sharply at this temperature; see Figure 13. This suggests that the cross-links supporting the connectivity network were suddenly released. Clear gels that are melted very slowly may exhibit some cloudiness *en route* to a clear melted state. This may be due to the formation of microgel aggregates as the connectivity network is undone. Another possibility is that phase separation processes may begin once the connectivity network is broken, in a process conceptually similar to the crystallization that occurs when a crystallizable polymer is warmed slightly above the glass transition temperature, after having first been rapidly cooled. The latter interpretation requires the liquid−liquid phase boundary to lie above the connectivity transition.

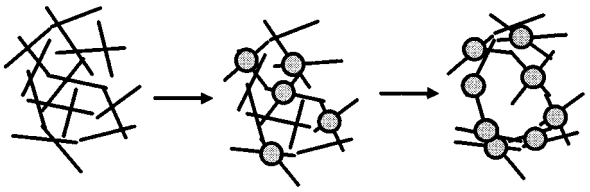

**Figure 14.** Proposed schematic representation of gelation for a cloudy gel. A clear gel may stop at the first step. Circles indicate zones of interaction among the rods that give rise to the DSC endotherms on melting.

A vexing problem is the difference in the present power law slopes for either clear or cloudy gels from those found for silica gels by Martin *et al.*[53,81] In their study of poly(methyl methacrylate) chemical gels, Fang, Brown, and Konak[74] found good agreement with the results of Martin *et al.*. Lang and Burchard[55] found an extended power law regime in thermoreversible gels of tamarind gum. The exponent $\phi$ on $t$ was somewhat ambiguously determined. From their Figure 2 (showing $g^{(1)}(q,t)$) one computes for $g^{(2)}(q,t)$ the value $\phi \approx 0.68$. However, the authors appear to draw a favorable comparison to the silica value of 0.27. If their Figure 2 is simply mislabeled regarding the order of the correlation function being displayed, that would account for a factor of 2 difference and the comparison would indeed be favorable. Ren and Sorensen[50] observed extended power law correlograms in gelatin and interpreted these results from the glass transition viewpoint. These authors also found a $q$ dependence for the power law exponent, an issue not addressed during the melting experiments of this paper.

## Summary

The DSC provides direct evidence for enthalpic interactions among the rods in PBLG/toluene gels, as inferred from earlier solution studies.[34] Whatever their molecular nature, the very presence of such interactions legitimizes an interpretation based partly on a connectivity transition. While phase separation is surely an important aspect of PBLG gelation in other solvents and also in some PBLG/toluene gels, it is not the only factor. The DSC results also mean that entanglements are not required to explain why phase separation stops, if once it does begin.

Apart from intensity, the scattering behavior of clear and cloudy gels was similar for the scattering vectors studied. We propose that cloudy gels begin as weakly connected networks which oppose, but not with complete success, microscopic phase separation at a later time. The phase separation may intensify rod−rod interactions. This would be consistent with the higher melting temperatures for 25 °C gels compared to the −10 °C gels of Figure 2. The proposed process for the cloudy gels is depicted in Figure 14. For rapidly quenched, clear gels, a more extensive percolation network may form that better resists the tendency toward phase separation. These observations underscore the importance of kinetics in gelation.

During the formation of the cloudy PBLG/toluene gels by slow, stepwise decreases in the temperature, the DLS experiments of Figures 7 and 8 did not identify a sharp gelation transition. Experiments conducted upon melting of clear and cloudy gels were more revealing. The power law behavior observed in chemical gels[53] was found near the melting point for both clear and cloudy gels. Although the power law regime extended for 3−5 decades of time, the power law slopes did not meet expectation.

## Conclusion

The PBLG/toluene system can exhibit a wide variety of behavior depending on gelation conditions. The hoped-for notion of universality in the gelation of rodlike polymers[6] is a casualty of the competition between connectivity and phase separation. Moreover, the interplay between these factors will depend on concentration, molecular weight, presence or absence of nucleating sites ("dust" which these samples lack), and cooling rate (a function of sample size and shape). As if this were not enough, another complexity lurks. Tanaka and Stockmayer point out that connectivity is akin to an order−disorder transition. In rodlike polymers, a real order−disorder transition between liquid phase exists. Its effect upon phase separation dynamics is beginning to get attention,[82−88] but theoretical treatments so far ignore the simple connectivity transition and sample history/kinetic effects. Although rodlike polymers are among the simplest structures known to form gels, they nevertheless exhibit a wealth of diverse behavior and complexity in doing so.

**Acknowledgment.** This work was supported by the National Science Foundation, DMR-9221585. Additionally, D.T. thanks the Louisiana Educational Quality Support Fund, administered by the Louisiana Board of Regents, for a fellowship to perform these studies under agreement NASA/LSU-(91-96)-01 and NASA/LaSPACE under grant NGT-40039. The DSC and ALV correlator were purchased with the assistance of the Louisiana Educational Quality Support Fund and Seiko USA. Finally, we are grateful to the referees for very helpful suggestions.

**Supporting Information Available:** Experimental details for light scattering sample preparation and DSC (3 pages). Ordering information is given on any current masthead page.

## References and Notes

(1) Bawden, F. C.; Pirie, N. W.; Bernal, J. D.; Fankuchen, I. *Nature* **1936**, *138*, 1051−1052.
(2) Tohyama, K.; Miller, W. G. *Nature* **1981**, *289*, 813−814.
(3) Sasaki, S.; Hikata, M.; Shiraki, C.; Uematsu, I. *Polym. J.* **1982**, *14* (3), 205−213.
(4) Russo, P. S.; Saunders, M. J.; Karasz, F. E. *Macromolecules* **1986**, *19*, 2856−2859.
(5) Cheng, S. Z. D.; Lee, S. K.; Barley, J. S.; Hsu, S. L. C.; Harris, F. W. *Macromolecules* **1991**, *24*, 1883−1889.
(6) Russo, P. S.; Chowdhury, A. H.; Mustafa, M. B. In *The Materials Science and Engineering of Rodlike Polymers*; Adams, W. W., Eby, R., McLemore, D., Eds.; Materials Research Society: Pittsburgh, PA, 1989; pp 207−222.
(7) Miller, W. G. *Annu. Rev. Phys. Chem.* **1978**, *29*, 519−535.
(8) Schmidt, M. *Macromolecules* **1984**, *17*, 553−560.
(9) Yamakawa, H. *Annu. Rev. Phys. Chem.* **1984**, *35*, 23−47.
(10) Helfrich, J.; Hentschke, R. *Macromolecules* **1995**, *28*, 3831−3841.
(11) DeLong, L. M.; Russo, P. S. *Macromolecules* **1991**, *24*, 6139−6155.
(12) Goebel, K. D.; Miller, W. G. *Macromolecules* **1970**, *3*, 64−69.
(13) Fujita, H.; Teramoto, A.; Yamashita, T.; Okita, K.; Ikeda, S. *Biopolymers* **1966**, *4*, 781−791.
(14) Wagner, N. J.; Walker, L. M.; Hammouda, B. *Macromolecules* **1995**, *28*, 5075−5081.
(15) Block, H. *Poly(γ-benzyl-L-glutamate) and other Glutamic Acid Containing Polymers*; Gordon and Breach: New York, 1983.
(16) Robinson, C. *Trans. Faraday Soc.* **1956**, *52*, 571−592.
(17) Robinson, C.; Ward, J. C.; Beevers, R. B. *Discuss. Faraday Soc.* **1958**, *25*, 29−42.
(18) Robinson, C. *Mol. Cryst.* **1966**, *1*, 467−494.
(19) Miller, W. G.; Wu, C. C.; Wee, E. L.; Santee, G. L.; Rai, J. H.; Goebel, K. G. *Pure Appl. Chem.* **1974**, *38*, 37−58.

(20) Russo, P. S.; Miller, W. G. *Macromolecules* **1983**, *16*, 1690−1693.
(21) Mead, D. W.; Larson, R. G. *Macromolecules* **1990**, *23*, 2524−2533.
(22) Burghardt, W. R.; Fuller, G. G. *Macromolecules* **1991**, *24* (9), 2546−2555.
(23) Kiss, G.; Porter, R. *J. Polym. Sci., Polym. Phys. Ed.* **1980**, *18*, 361−388.
(24) Miller, W. G.; Lee, K.; Tohyama, K.; Voltaggio, V. *J. Polym. Sci., Polym. Symp.* **1978**, *65*, 91−106.
(25) Russo, P. S.; Magestro, P.; Miller, W. G. In *Reversible Polymeric Gels and Related Systems*; Russo, P. S., Ed.; American Chemical Society: Washington, 1987; pp 153−180.
(26) Chowdhury, A. H.; Russo, P. S. *J. Chem. Phys.* **1990**, *92* (9), 5744−5750.
(27) Ginzburg, B.; Siromyatnikova, T.; Frenkel, S. *Polym. Bull. (Berlin)* **1985**, *13*, 139−144.
(28) Pluyter, J. G. L.; Samulski, E. T. *ACS Polym. Prepr. (Am. Chem. Soc., Div. Polym. Chem.)* **1991**, *32*, (1), 140−141.
(29) Cohen, Y.; Dagan, A. *Macromolecules* **1995**, *28*, 7638−7644.
(30) Shukla, P.; Muthukumar, M.; Langley, K. H. *J. Appl. Polym. Sci.* **1992**, *44*, 2115−2125.
(31) Shukla, P.; Muthukumar, M. *J. Polym. Sci., Polym. Phys. Ed.* **1991**, *29*, 1373−1387.
(32) Donald, A. M.; Horton, J. C. *Polymer* **1991**, *32* (13), 2418−2427.
(33) Prystupa, D. A.; Donald, A. M. *Macromolecules* **1993**, *26*, 1947−1955.
(34) Chakrabarti, S.; Miller, W. G. *Biopolymers* **1984**, *23*, 719−734.
(35) Kyu, T.; Mukherjee, P. *Liq. Cryst.* **1988**, *3*, 631−644.
(36) Flory, P. J. *Proc. R. Soc. London, Ser. A* **1956**, *234*, 60−73.
(37) Flory, P. J. *Proc. R. Soc. London, Ser. A* **1956**, *234*, 73−89.
(38) Cohen, Y.; Buchner, S.; Zachmann, H. G.; Davidov, D. *Polymer* **1992**, *33*, 3811−3817.
(39) Russo, P. S. Unpublished results.
(40) Edwards, S. F.; Evans, K. E. *Trans. Faraday Soc.* **1982**, *78*, 113−121.
(41) Edwards, S. F. *Polymer* **1994**, *35*, 3827−3830.
(42) Bu, Z.; Russo, P. S.; Tipton, D. L.; Negulescu, I. I. *Macromolecules* **1994**, *27*, 6871−6882.
(43) Tanaka, T.; Hocker, L. O.; Benedek, G. B. *J. Chem. Phys.* **1973**, *59*, 5151−5159.
(44) Stauffer, D.; Coniglio, A.; Adam, M. In *Polymer Networks*; Advances in Polymer Science Vol. 44; Dusek, K., Ed.; Springer-Verlag: Berlin, 1982; pp 105−158.
(45) Stauffer, D. *Introduction to Percolation Theory*; Taylor and Francis: London, 1985.
(46) Coniglio, A.; Stanley, H. E.; Klein, W. *Phys. Rev. B* **1982**, *25*, 6805−6821.
(47) Matsuo, E. S.; Orkisz, M.; Sun, S.-T.; Li, Y.; Tanaka, T. *Macromolecules* **1994**, *27*, 6791−6796.
(48) The commonly experienced "melt crystallization" of rapidly glassed polymers upon heating is conceptually similar.
(49) Arnauts, J.; Berghmans, H. *Polym. Commun.* **1987**, *28*, 66−68.
(50) Ren, S. Z.; Sorensen, C. M. *Phys. Rev. Lett.* **1993**, *70*, 1727−1730.
(51) Tanaka, F.; Stockmayer, W. H. *Macromolecules* **1994**, *27*, 3943−3954.
(52) Schatzel, K. In *Dynamic Light Scattering, The Method and Some Applications*; Brown, W., Ed.; Oxford University Press: New York, 1993; pp 76−148.
(53) Martin, J. E.; Wilcoxon, J.; Odinek, J. *Phys. Rev. A* **1991**, *43* (2), 858−872.
(54) Pusey, P. N. *Macromol. Symp.* **1994**, *79*, 17−30.
(55) Lang, P.; Burchard, W. *Macromolecules* **1991**, *24*, 814−815.
(56) Joosten, J. G. H.; McCarthy, J. L.; Pusey, P. N. *Macromolecules* **1991**, *24*, 6690−6699.
(57) Pusey, P. N.; Van Megen, W. *Physica A* **1989**, *157*, 705−741.
(58) Berne, B.; Pecora, R. *Dynamic Light Scattering*; Wiley: New York, 1976.
(59) Chu, B. *Laser Light Scattering*; Academic Press: New York, 1991.
(60) Ford, N. C. In *Dynamic Light Scattering*; Pecora, R., Ed.; Plenum: New York, 1985; pp 7−58.
(61) Russo, P. S.; Miller, W. G. *Macromolecules* **1984**, *17*, 1324−1331.
(62) Guenet, J. M. *Thermoreversible Gelation of Polymers and Biopolymers*; Academic Press: New York, 1992; Chapter 1.
(63) Guenet, J. M.; McKenna, G. B. *Macromolecules* **1988**, *21*, 1752−1756.
(64) Doty, P.; Bradbury, J. H.; Holtzer, A. M. *J. Am. Chem. Soc.* **1956**, *78*, 947−954.
(65) Richards, E. G. An *Introduction to the Physical Properties of Large Molecules in Solution*; Cambridge University Press: New York, 1980.
(66) Newman, J.; Mroczka, N.; Schick, K. L. *Macromolecules* **1989**, *22*, 1006−1008.
(67) Schmidt, P. W. In *The Fractal Approach to Heterogeneous Chemistry*: *Surfaces, Colloids, Polymers*; Avnir, D., Ed.; Wiley: New York, 1989; pp 55−66.
(68) Dadmun, M. A.; Muthukumar, M.; Han, C. C.; Hempelmann, R.; Schwahn, D.; Springer, T. *Macromolecules* **1996**, *29*, 207−211.
(69) Tadmor, R.; Cohen, Y. *J. Phys. IV* **1993**, *3*, 103−106.
(70) Cohen, Y.; Talmon, Y.; Thomas, E. L. In *Physical Networks Polymers and Gels*; Burchard, W., Ross-Murphy, S. B., Eds.; Elsevier: London, 1990; pp 147−158.
(71) Ferry, J. D. *Viscoelastic Properties of Polymers*; Wiley: New York, 1980; Chapter 17.
(72) Tipton, D. L. Ph.D. Thesis, Louisiana State University, 1995.
(73) Brenner, S. L.; Gelman, R. A.; Nossal, R. *Macromolecules* **1978**, *11*, 202−212.
(74) Fang, L.; Brown, W.; Konak, C. *Macromolecules* **1991**, *24*, 6839−6842.
(75) Wong, A. P.; Wiltzius, P. *Rev. Sci. Instrum.* **1993**, *64*, 2547−2549.
(76) Stepanek, P. In *Dynamic Light Scattering, The Method and Some Applications*; Brown, W., Ed.; Clarendon Press: Oxford, U.K., 1993; pp 175−241.
(77) Provencher, S. W. *Comput. Phys.* **1982**, *27*, 213−227.
(78) Provencher, S. W. *Comput. Phys.* **1982**, *27*, 229−242.
(79) Russo, P. S.; Saunders, M. J.; DeLong, L. M.; Kuehl, S. K.; Langley, K. H.; Detenbeck, R. W. *Anal. Chim. Acta* **1986**, *189*, 69−87.
(80) Ostrowski, N.; Sornette, D.; Parker, P.; Pike, E. R. *Opt. Acta* **1981**, *28*, 1059−1070.
(81) Martin, J. E.; Wilcoxon, J. *Phys. Rev. Lett.* **1988**, *61*, 373−376.
(82) Doi, M.; Shimada, T.; Okano, K. J. *J. Chem. Phys.* **1988**, *88*, 4070−4075.
(83) Shimada, T.; Doi, M.; Okano, K. J. *J. Chem. Phys.* **1988**, *88*, 2815−2821.
(84) Shimada, T.; Doi, M.; Okano, K. *J. Chem. Phys.* **1988**, *88*, 7181−7186.
(85) Dorgan, J. R. *J. Chem. Phys.* **1993**, *98*, 9094−9106.
(86) Wong, A. P.; Wiltzius, P.; Larson, R. G.; Yurke, B. *Phys. Rev. E* **1993**, *47*, 2683−2688.
(87) Chuang, I.; Turok, N.; Yurke, B. *Phys. Rev. Lett.* **1991**, *66*, 2472−2475.
(88) Bray, A. J.; Puri, S. *Phys. Rev. Lett.* **1991**, *67*, 2670−2673.

MA960029G